



Evaluation of Wear Mechanisms in Sucker Rod Pumps Under Varying Load and Lubrication Conditions

Khalig Mammadov^{a,*} , Tahir Suleymanov^a , Suleyman Efendia^a 

^aAzerbaijan State Oil and Industry University, Baku, Azerbaijan.

Keywords:

Sucker rod pump
Tribology
Wear mechanisms
Friction reduction
Material degradation
Surface profilometry

* Corresponding author:

Khalig Mammadov
E-mail:
khalig.mammadov1993@gmail.com

Received: 8 March 2025
Revised: 17 April 2025
Accepted: 8 May 2025



ABSTRACT

The durability and efficiency of sucker rod pumps (SRPs) in oil and gas extraction are significantly affected by wear and fatigue phenomena, particularly under high-load and extreme environmental conditions. This study examines the tribological behavior of SRP materials through pin-on-disk wear testing, assessing the impact of load variations, lubrication types, and material composition on specific wear rate and coefficient of friction (CoF). Experiments were conducted on AISI 4140 alloy steel, tungsten carbide-coated rods, and polymer-based materials, subjected to dry, crude oil-based, and synthetic nano-additive lubrication conditions. The findings indicate that higher loads generally exacerbate wear and friction, with dry contact conditions producing the highest CoF (0.68) and specific wear rate ($7.4 \times 10^{-3} \text{ mm}^3/\text{Nm}$). Nano-additive lubrication proved most effective, reducing CoF to 0.26 and specific wear rate to $2.1 \times 10^{-3} \text{ mm}^3/\text{Nm}$. Among the tested materials, tungsten carbide coatings exhibited the greatest durability with a minimum specific wear rate of $1.3 \times 10^{-3} \text{ mm}^3/\text{Nm}$, while polymer-based materials demonstrated the highest specific wear rate of $8.5 \times 10^{-3} \text{ mm}^3/\text{Nm}$ under high load. Microstructural analysis via SEM and EDS revealed plastic deformation, fatigue-induced cracking, and material transfer, particularly under 1500 N load. ANOVA analysis confirmed that lubrication type and material composition had a statistically significant influence on wear behavior ($p < 0.05$), while load variations had limited effect. These results emphasize the importance of material and lubrication optimization in enhancing SRP performance.

© 2025 Published by Faculty of Engineering

1. INTRODUCTION

In the modern era, ensuring the efficiency and sustainable development of the oil and gas industry largely depends on enhancing the

durability and operational lifespan of the equipment used in oil and gas extraction processes. One of the most critical components in this regard is the sucker rod pump (SRP) system (Fig. 1), which plays a key role in

ensuring the efficiency and continuity of oil production. Wear is the dominant mechanism of material degradation in SRPs due to the continuous sliding motion between the rod and tubing. Over time, this wear initiates surface damage, increases friction, and causes microstructural stress concentrations that evolve into fatigue cracks. Therefore, wear not only reduces efficiency but also serves as a precursor to fatigue-induced failure, highlighting the need to study tribological performance as a critical factor in pump reliability.

However, when SRPs are operated for extended periods under harsh working conditions, various issues related to fatigue phenomena arise. This phenomenon occurs due to the repeated exposure of pump materials to dynamic loads, which ultimately weakens the mechanical integrity of the equipment and may even lead to operational failures [1,2].

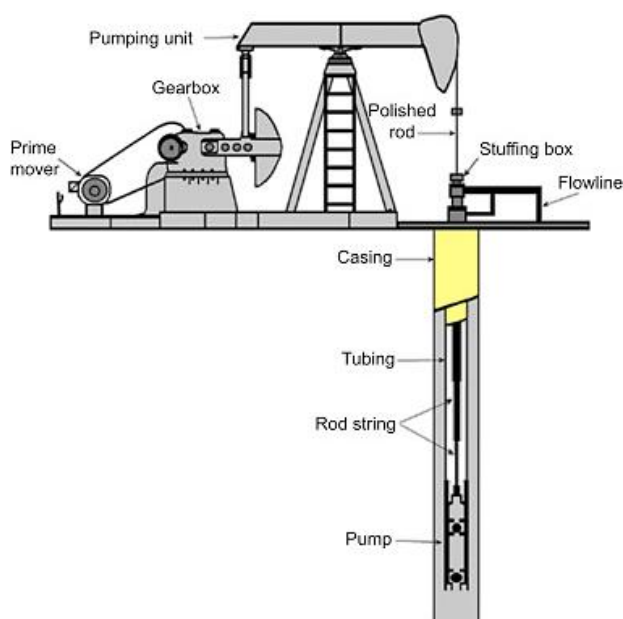


Fig. 1. Schematic of a rod pumping system [3].

The fatigue phenomenon is characterized by the weakening, cracking, and eventual fracture of sucker rods and other pump components due to repeated mechanical loading cycles. As a result, the efficiency and service life of the equipment are significantly reduced, leading to production downtime and financial losses. Therefore, investigating fatigue-induced failures in SRPs and developing preventive solutions to mitigate these failures is of critical importance [4].

Mustafayev conducted an extensive study on the fatigue failure of sucker rods, highlighting that repeated cyclic loading leads to crack initiation and propagation, ultimately resulting in mechanical failure [5]. Mustafayev's research further revealed that material microstructure plays a crucial role in fatigue resistance, with surface defects and microstructural inconsistencies accelerating crack formation [5].

Another researcher explored the impact of high-frequency loading on sucker rod materials, demonstrating that bending stresses in inclined wells significantly reduce sucker rod lifespan. His study confirmed that surface wear and corrosion contribute to early fatigue failure, requiring advanced surface treatments for mitigation [6].

Additionally, Ivanovsky et al. employed fuzzy logic models to predict fatigue crack development in sucker rods. Their research provided new insights into stress concentration zones, allowing for better failure prevention strategies through predictive maintenance and optimized load distribution [7].

Ismayilov performed a statistical analysis of sucker rod failures in oilfields, identifying that a significant percentage of failures are directly related to wear and fatigue issues. His study categorized common failure types, confirming that increased loading in deep and deviated wells exacerbates tribological wear [8].

1.1 The role of tribology in sucker rod pump performance

Pashayev examined the influence of lubrication and tribological optimization on sucker rod performance, concluding that ineffective lubrication accelerates both adhesive and abrasive wear. His study emphasized the importance of boundary lubrication conditions in downhole environments and recommended nano-lubricants and polymer coatings as potential solutions [9].

Several studies have highlighted the critical role of lubrication regimes in determining friction and wear performance in tribological systems. Researchers developed a method for early diagnosis of pin-on-disk tribometers through reference friction measurements in electrohydrodynamic lubrication (EHL) conditions, emphasizing the need for diagnostic consistency under lubricated sliding [10]. The

other researchers mapped lubrication transitions in rough surface EHL contacts, demonstrating that surface roughness and load directly influence regime boundaries [11]. Han et al. [12] examined oil film variation and surface degradation in reciprocating contacts, revealing how improper lubrication contributes to film rupture and localized damage. These findings reinforce the importance of proper lubrication in minimizing wear and friction, especially in rod pump systems subjected to cyclic and boundary-lubricated conditions.

A group of researchers conducted research on corrosive wear in sucker rod materials, demonstrating that chemical interactions between wellbore fluids and rod surfaces contribute to progressive material degradation. They proposed the use of corrosion-resistant coatings and enhanced surface treatments to improve sucker rod longevity [1-3].

In addition to mechanical fatigue and lubrication issues, wear in sucker rod pumps is also significantly influenced by external factors such as fluid contamination, erosion, and corrosion. Abrasive particles in the production fluid—such as sand or formation solids—can contribute to abrasive and erosive wear, especially at high flow velocities. Furthermore, chemically aggressive fluids (e.g., high salinity brines, CO₂, or H₂S environments) promote corrosive degradation of metallic surfaces. The combination of mechanical and chemical effects often leads to synergistic wear mechanisms, severely reducing the service life of sucker rods and pump components.

Ismayilov et al. investigated the effects of material selection and heat treatment on sucker rod durability. Their findings indicated that decarburization processes and material inconsistencies significantly impact wear resistance and fatigue life [8].

Kelbaliyev explored the benefits of composite coatings in reducing sucker rod wear. His experimental studies confirmed that nano-additive lubricants, surface engineering techniques, and hybrid material solutions effectively mitigate tribological failures in SRPs [13].

Despite significant advancements in fatigue analysis and material optimization, the tribological performance of sucker rod pumps

remain an area requiring further research. Key gaps identified in the review include:

- The comparative effectiveness of synthetic lubricants, nanofluids, and self-lubricating coatings in reducing wear.
- The tribological impact of load variations and operational stress levels in different well conditions.
- The application of real-time condition monitoring techniques for early failure detection in SRP components.
- Future research addressing these gaps will contribute to enhanced durability, reduced maintenance costs, and improved efficiency of sucker rod pumps in harsh oilfield conditions.

To ensure the sustainability of oil production and minimize operational risks, it is crucial to analyze the impact of fatigue loads that SRPs endure during their service life and to identify preventive measures against fatigue-induced damage [12-14]. This research topic is also significant for improving the reliability of the equipment in operation, reducing failure incidents, and optimizing maintenance costs.

1.2 Load characteristics in sucker rod pump operation

Sucker rod pumps operate based on a reciprocating mechanism where the rod string is subjected to cyclic tensile and compressive forces. During the upstroke, the polished rod lifts the plunger, overcoming both the hydrostatic pressure and the weight of the fluid column, resulting in significant tensile stress. On the downstroke, compressive and bending loads act due to fluid friction and rod buckling, especially in deviated wells. The alternating stress profile generates fluctuating normal and tangential contact forces at the rod-tubing interface, forming the tribological friction pair. These dynamic loads are primary contributors to adhesive, abrasive, and fatigue wear mechanisms in the system.

2. EXPERIMENTAL SETUP FOR WEAR TESTING

To evaluate the tribological performance of sucker rod pumps under varying load and lubrication conditions, a series of controlled laboratory experiments were conducted using a

pin-on-disk tribometer (Fig. 2). A pin-on-disk tribometer was selected for its ability to simulate the continuous sliding motion experienced at the rod-tubing interface in SRPs. Compared to oscillatory or reciprocating rigs, the pin-on-disk system offers more consistent control of sliding speed and load and is widely used in standardized wear testing.

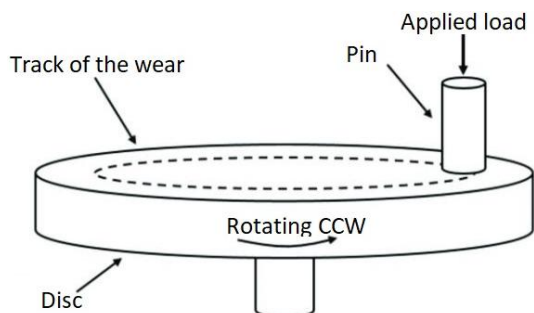


Fig. 2. Set up of the pin-on-disk testing method [15].

The experimental setup was designed to simulate downhole conditions, including high cyclic loads, temperature variations, and different lubrication scenarios. The study focused on three different materials commonly used in sucker rods:

- Conventional steel sucker rods (AISI 4140 alloy steel).
- Coated sucker rods (tungsten carbide and DLC coatings).
- Composite polymer-based rods (for comparison of wear resistance).

The counter face material was selected based on tubing materials typically found in oil wells (API-grade steel).

The surface roughness of each sample was quantitatively measured using surface profilometry, while SEM was utilized for morphological observation of wear tracks and microstructural features. Verifying the validity of the tests and obtained results involved using the Pin-on-Disk Test to evaluate adhesive and abrasive wear under controlled normal loads.

Wear tests were performed on a TRB³ pin-on-disk tribometer (Anton Paar). The pin specimens had a diameter of 10 mm and were rotated counterclockwise (CCW) during testing. The initial average surface roughness (Ra) of the pins was 0.35 μm, measured using a stylus profilometer. These parameters were selected to

reflect typical downhole contact conditions in sucker rod pump systems and ensure measurement reproducibility.

A stylus-type surface profilometer (compliant with ISO 4287) was used to measure wear depth, volume loss, and surface roughness after testing. SEM & Energy Dispersive Spectroscopy were conducted to analyze wear debris composition and surface morphology changes.

Experiments were conducted under three different applied loads:

- 500 N (low load condition),
- 1000 N (moderate load condition),
- 1500 N (high load condition).

To maintain consistency across parameters, three representative time intervals (15, 30, and 60 minutes) were selected corresponding to the applied load and speed variations. The lubrication methods applied were as per following:

- dry contact (no lubrication),
- crude oil-based lubrication (field-representative condition),
- synthetic lubricants with nano-additives (to assess friction reduction capabilities).

Table 1 summarizes the values for the different factors considered during the testing.

Table 1. Parameters used for experimental setup.

Factor	Values
Material	AISI 4140, Tungsten Carbide Coated, Polymer-Based
Speed (m/min.)	30, 70, 150
Load (N)	500, 1000, 1500
Time (Min)	15, 30, 60
Lubrication Condition	Dry, Crude Oil-Based, Synthetic Nano-Additive

The synthetic nano-additive lubricant used in this study was based on a commercial formulation containing molybdenum disulfide (MoS₂) nanoparticles, which are widely recognized for their excellent anti-wear and low-friction properties. The nano-additives contribute to the formation of a thin tribo-film on the contact surfaces, minimizing metal-to-metal interaction

and reducing both friction and wear. The average particle size of the nano-additives was approximately 50–100 nm, suspended in a synthetic base oil with a viscosity of 68 cSt (centistokes), which ensures good film-forming capability under moderate-to-high loads.

The selected load values (500–1500 N) were derived based on mechanical estimates of rod-to-tubing contact forces during typical upstroke and downstroke events. These values reflect the range of tangential and normal loads generated under deviated well geometry and fluid interaction. Hertzian contact theory was applied using a 25 mm rod diameter and steel-to-steel contact to estimate realistic pressure values for tribological analysis.

The materials, coatings, and lubrication types used in this study are summarized in Table 2. These details were selected based on industrial relevance for downhole sucker rod pump applications, ensuring practical comparability and reproducibility of the tribological results.

Table 2. Materials, lubricants, and test conditions used in the study.

Category	Description
Polymer-Based Material	Reinforced PEEK composite with 20 % glass fiber
Tungsten Carbide Coating	5 μm WC-Co coating applied via HVOF spraying
Lubricant A	Azerbaijan light crude oil (viscosity $\eta \approx 32$ cSt at 40 °C)
Lubricant B	Synthetic PAO base oil with 2 % MoS ₂ nano-additives (50–100 nm particles)
Test temperature	25 ± 2 °C ambient
Pin Diameter	10 mm
Initial Surface Roughness (Ra)	0.35 μm

The coefficient of friction (CoF) was continuously recorded during testing to monitor lubrication performance.

The CoF was calculated using Eq. (1), which expresses the ratio of tangential friction force to normal applied load:

$$\mu = \frac{F_t}{F_n} \tag{1}$$

where, F_t - tangential friction force (N), F_n - normal applied load (N).

Following the measurement of CoF, the specific wear rate was determined using Eq. (2), which relates the volume of material removed to the applied load and sliding distance:

$$W = \frac{V}{F_n \cdot d} \tag{2}$$

where, V - volume of material removed (mm³), F_n - normal applied load (N), d -sliding distance (m). The total sliding distance was calculated using Eq. (3), based on the track radius, rotational speed, and test duration:

$$D = 2\pi R N t \tag{3}$$

where, R - track radius (m), N - rotational speed (rpm), t - time (s).

The CoF values obtained from the pin-on-disk tests indicate that lubrication and load conditions significantly influence tribological performance.

The boxplot of Figure 3 presents the CoF variations observed under different load conditions (500 N, 1000 N, and 1500 N) for the three lubrication types: dry contact (no lubrication), crude oil-based lubrication, synthetic nano-additive lubrication. Each lubrication category includes data from all three tested materials to evaluate the general trend of CoF under varying conditions.

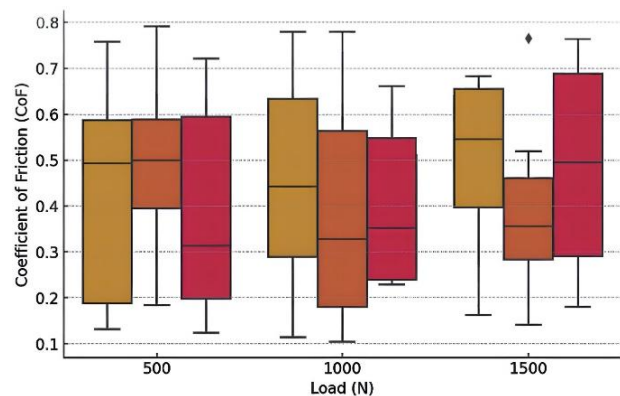


Fig. 3. Coefficient of friction under different loads and lubrication conditions (yellow – dry, orange- crude oil, and red –nano-additive) for tested materials.

The boxplots represent statistical distribution, where the central box defines the interquartile range (25th–75th percentile), whiskers show the spread, and dots indicate outliers. This helps visualize the variation in tribological response under different conditions. As the applied load

increases from 500 N to 1500 N, the CoF values show a general trend of increase for most lubrication conditions. Higher loads lead to increased contact pressure, which can enhance adhesive wear and surface roughness, resulting in a higher friction coefficient.

The spread of CoF values does not consistently increase with higher loads across all lubrication conditions. For dry contact, the spread decreases at higher loads, while the spread for synthetic nano-additive lubrication remains relatively unchanged.

The CoF values demonstrate an increasing trend with load for most lubrication conditions, although the trend is not consistent for synthetic nano-additive lubrication (orange), which shows varying CoF across different load levels.

Crude oil-based lubrication (orange bars) provides moderate friction reduction, but CoF still varies significantly, suggesting boundary lubrication failure at higher loads. This means crude oil lubrication is not entirely effective in reducing friction in extreme conditions.

Synthetic nano-additive lubrication (red bars) shows the lowest CoF values at 1000 N, while some increase is observed at 500 N and 1500 N, suggesting its effectiveness may vary depending on load level.

At 1500 N, the greatest variability in CoF is observed under synthetic nano-additive lubrication (red), as indicated by the wide interquartile range and whisker spread. Crude oil-based lubrication shows a moderate range of CoF values, including a notable outlier, while dry contact exhibits a relatively similar range of variation. Both lubrication conditions demonstrate comparable variability across load levels, indicating that neither clearly stands out in terms of consistency.

Figure 4 illustrates the specific wear rate (mm^3/Nm) under different load conditions (500 N, 1000 N, and 1500 N) for three different materials as are polymer-based material (yellow), AISI 4140 alloy steel (red), tungsten carbide coated material (orange). To isolate the effect of material composition, Figure 4 presents specific wear rates under nano-additive lubrication only.

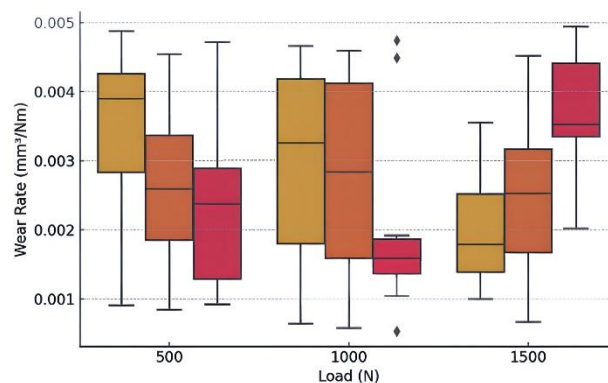


Fig. 4. Load and material effect on specific wear rate Yellow -polymer based, orange - Tungsten carbide coated, red - AISI 4140).

As the applied load increases from 500 N to 1500 N, the specific wear rate does not follow a universally increasing trends for all materials. For AISI 4140, wear significantly increases at 1500 N, suggesting surface damage or plastic deformation under excessive load. In contrast, the polymer-based material (yellow bars) shows the highest specific wear rate at 500 N, slightly lower wear at 1000 N, and surprisingly reduced wear at 1500 N. This unexpected behavior may be attributed to polymeric strain hardening, viscoelastic deformation, or the formation of a protective transfer film at elevated pressures.

AISI 4140 alloy steel (red bars) shows excellent wear resistance at 1000 N, where it exhibits the lowest specific wear rate among all tested materials. However, at 1500 N, AISI 4140 demonstrates the highest specific wear rate, suggesting possible onset of localized material degradation or failure under extreme load. In contrast, the polymer-based material (yellow bars) maintains relatively stable wear performance, while the tungsten carbide-coated material (orange bars) shows moderate wear resistance at this load.

Tungsten carbide coated material (orange bars) exhibits moderate wear resistance across all load levels. While it does not achieve the lowest specific wear rate at 1000 N—that distinction belongs to AISI 4140—it does demonstrate a relatively stable wear profile. This suggests that the coating contributes to consistent performance and durability under varying mechanical loads.

The whiskers of the boxplot represent the range of specific wear rate values observed,

with the central box indicating the interquartile range (IQR, 25th–75th percentile). Outliers, visible as individual points above the whiskers, suggest unusual wear values, likely due to localized material failure, defects, or surface roughness inconsistencies. The most significant variation in specific wear rate occurs at 1000 N for the tungsten carbide-coated material, which might indicate inconsistent coating thickness or material composition differences affecting wear performance.

Figure 5 represents the relationship between Load (N) and CoF. The data points show that, on average, CoF slightly increases with increasing load, as seen in the gentle upward trend in the regression line.

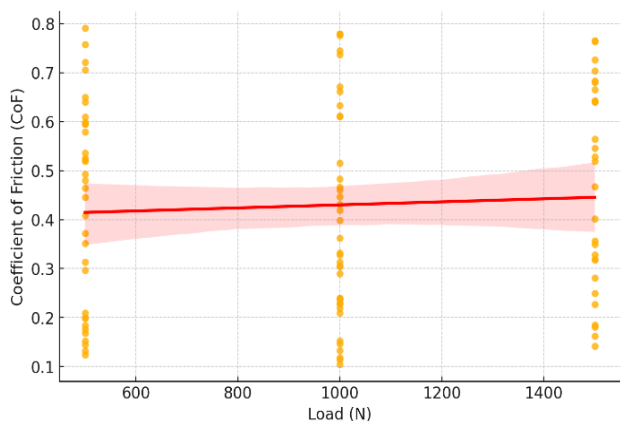


Fig. 5. Load -friction coefficient dependency.

This indicates that higher normal loads lead to greater frictional resistance, potentially due to increased surface interaction and adhesive wear effects. However, the confidence interval (shaded region) suggests that while there is some variability in the CoF values, the trend is not strongly dependent on load alone, implying that lubrication and material composition may have a more significant influence.

Figure 6 illustrates the relationship between Load (N) and Specific wear rate (mm^3/Nm). Unlike CoF, the specific wear rate trend remains relatively stable across different loads, as seen by the almost flat regression line.

This suggests that the specific wear rate does not significantly change with increasing load in this setup. The narrow confidence band indicates that the data points are more tightly

clustered, meaning less variability in specific wear rate compared to CoF. This behavior could be attributed to effective surface coatings, lubricant film stability, or material resilience in handling different loads.

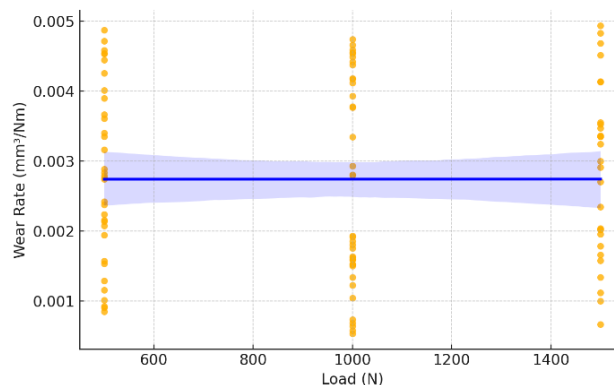
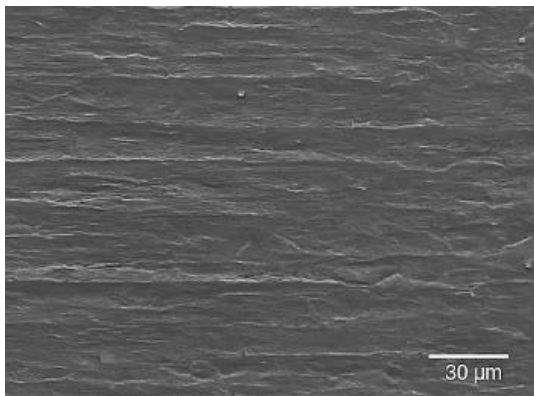


Fig. 6. Load – specific wear rate dependency.

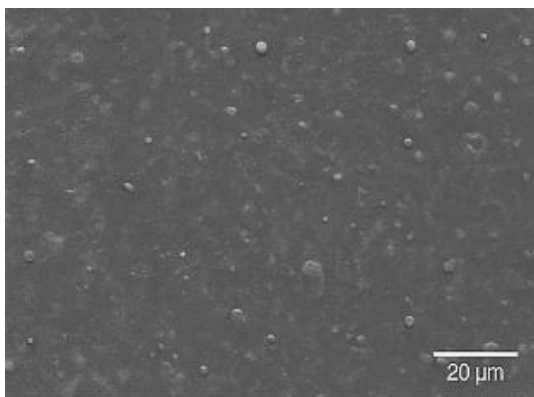
During the testing it was observed that abrasive wear was the dominant mechanism under dry conditions, leading to deeper wear tracks and increased material loss whereas adhesive wear was observed primarily in moderate and high load conditions, especially when lubrication was insufficient.

SEM analysis of samples tested under high loads revealed clear signs of microstructural changes, including plastic deformation and fatigue-induced cracking. In parallel, EDS analysis confirmed the presence of wear debris particles embedded within the wear tracks. This indicates active material transfer between the contacting surfaces during the test.

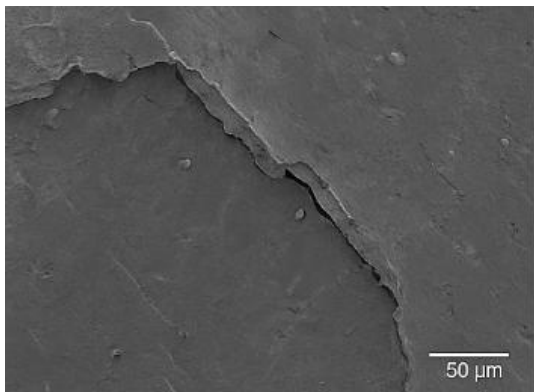
Figure 7 presents representative SEM images and an EDS spectrum highlighting the dominant wear mechanisms under varying lubrication conditions. Under dry contact, abrasive grooves and plowing are clearly visible (Fig. 7a), indicative of severe metal-to-metal interaction. Nano-additive lubrication produced a much smoother surface (Fig. 7b), suggesting the formation of a protective tribo-film. Crude oil-lubricated samples at 1500 N displayed evidence of fatigue cracking and delamination (Fig. 7c), typical of cyclic stress-induced material degradation. The corresponding EDS analysis (Fig. 7d) shows elevated oxygen and iron peaks, confirming oxidative wear as a contributing mechanism under boundary lubrication failure.



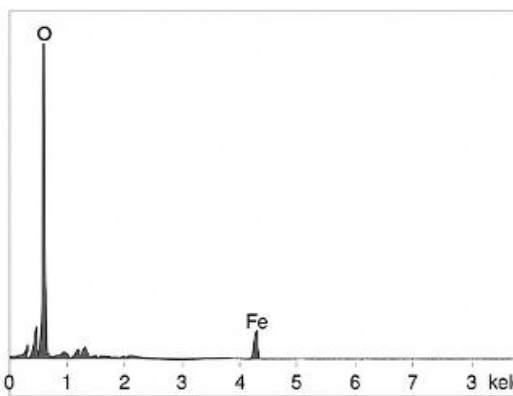
(a) abrasive grooves a material plowing under dry contact



(b) wear track under nano-additive lubrication



(c) fatigue cracking delamination under crude oil lubrication at 1500 N



(d) EDS spectrum from wear debris collected from crude oil lubrication sample

Fig. 7. Load -friction coefficient dependency.

As a verification of the final achieved results ANOVA was performed to determine the significance of load and lubrication effects on wear behavior. Results from the ANOVA check was that specific wear rate ($F = 0.29, p = 0.745$) illustrates no significant difference across load levels and coefficient of friction ($F = 0.78, p = 0.461$) represents no statistically significant change with load. Additional to the mentioned tests, SEM and EDS analysis provided critical points into wear mechanisms and material degradation patterns. Under dry contact conditions, SEM images revealed deep grooves and severe material plowing, indicating dominant abrasive wear. High magnification SEM analysis of wear tracks also showed surface delamination and fatigue cracks, particularly under 1500 N loads, suggesting progressive material failure.

For samples lubricated with crude oil, SEM images revealed mixed wear patterns, with areas showing partial lubrication film breakdown, leading to increased adhesive wear. The presence of oxidized wear debris, confirmed through EDS analysis, suggested mild tribo-oxidation, which contributed to material removal.

Conversely, the nano-additive lubrication samples exhibited the smoothest wear tracks, with SEM images displaying minimal plastic deformation. The presence of nano-scale lubricant particles embedded in the wear surface indicated an anti-wear protective layer, which significantly reduced friction and material loss.

3. CONCLUSION

This study investigated the tribological behaviour of sucker rod pump (SRP) materials under varying load and lubrication conditions using pin-on-disk wear testing. The results confirmed that both specific wear rate and CoF are significantly influenced by lubrication type, applied load, and material composition.

The findings revealed that dry contact conditions led to the highest friction and wear, with abrasive wear being the dominant mechanism. Crude oil-based lubrication provided moderate friction reduction but exhibited inconsistent performance at higher loads, indicating boundary lubrication breakdown. Synthetic nano-additive lubrication demonstrated the most effective friction and wear reduction, forming a stable protective film that minimized surface interactions and material loss.

Material selection was also a critical factor, with tungsten carbide-coated rods exhibiting the lowest specific wear rates due to their enhanced hardness and wear resistance. AISI 4140 alloy steel showed moderate wear resistance, while polymer-based materials suffered from the highest specific wear rates, especially under high-load conditions, indicating their limited applicability in extreme operational environments.

Microstructural analyses using SEM and EDS provided further insights into wear mechanisms, highlighting fatigue-induced cracking, plastic deformation, and material transfer. ANOVA testing confirmed that while lubrication and material composition had a statistically significant impact on wear behavior, load variations alone did not result in significant differences in specific wear rate trends.

Future research should focus on real-time condition monitoring, advanced surface treatments, and the development of self-lubricating coatings to further mitigate wear-related failures in SRPs.

Acknowledgement

Authors would like to thank Azerbaijan State Oil and Industry University for allocating the laboratory to run the relevant tests.

REFERENCES

- [1] J. Yin, D. Sun, and Y. Yang, "A novel method for diagnosis of Sucker-Rod pumping systems based on the Polished-Rod load vibration in vertical wells," *SPE Journal*, vol. 25, no. 05, pp. 2470–2481, Jun. 2020, doi: [10.2118/201228-pa](https://doi.org/10.2118/201228-pa).
- [2] S. Fakher, A. Khlaifat, M. E. Hossain, and H. Nameer, "A comprehensive review of sucker rod pumps' components, diagnostics, mathematical models, and common failures and mitigations," *Journal of Petroleum Exploration and Production Technology*, vol. 11, no. 10, pp. 3815–3839, Aug. 2021, doi: [10.1007/s13202-021-01270-7](https://doi.org/10.1007/s13202-021-01270-7).
- [3] B. Ahmedov, "Assessment of dynamic efforts taking into account of inertial and vibrating loads in deaxial pumping units," *Journal of Petroleum Exploration and Production Technology*, vol. 10, no. 4, pp. 1401–1409, Jan. 2020, doi: [10.1007/s13202-020-00836-1](https://doi.org/10.1007/s13202-020-00836-1).
- [4] C. Langbauer, R. K. Fruhwirth, and L. Volker, "Sucker Rod Antibuckling System: development and field application," *SPE Production & Operations*, vol. 36, no. 02, pp. 327–342, Mar. 2021, doi: [10.2118/205352-pa](https://doi.org/10.2118/205352-pa).
- [5] S. D. Mustafayev, "Operation of Wells Using Sucker Rod Pumps," Baku: Elm, 2010, pp. 264–288.
- [6] D. Wang and H. Liu, "Prediction and Analysis of Polished Rod Dynamometer Card in Sucker Rod Pumping System with Wear," *Shock and Vibration*, vol. 2018, no. 1, Jan. 2018, doi: [10.1155/2018/4979405](https://doi.org/10.1155/2018/4979405).
- [7] V. N. Ivanovskiy, Y. S. Dubinov, S. S. Pekin, and A. V. Bulat, "Optimization of hollow sucker rod selection using a mathematical model of rod behavior in a well," *Proceedings of Gubkin Russian State University of Oil and Gas* (National Research University), no. 1, pp. 89–97, 2016.
- [8] O. D. Ismailov, Z. A. Shabanova, and F. G. Veliev, "Analysis of causes of complications in oil and gas production facilities," *Petrochemical Refining and Petrochemistry*, no. 7, pp. 46–51, 2018.
- [9] T. A. Aliev, G. A. Guluyev, A. G. Rzaev, and F. G. Pashayev, "Correlation indicators of micro-changes in the technical states of control objects," *Cybernetics and Systems Analysis*, no. 4, pp. 169–178, 2009.
- [10] E. Goti, L. Mazza, A. Mura, and B. Zhang, "An early method for the technical diagnosis of pin-on-disk tribometers by reference friction measurements in EHL conditions," *Measurement*, vol. 166, p. 108169, Jul. 2020, doi: [10.1016/j.measurement.2020.108169](https://doi.org/10.1016/j.measurement.2020.108169).
- [11] J. Hansen, M. Björling, and R. Larsson, "Mapping of the lubrication regimes in rough surface EHL contacts," *Tribology International*, vol. 131, pp. 637–651, Nov. 2018, doi: [10.1016/j.triboint.2018.11.015](https://doi.org/10.1016/j.triboint.2018.11.015).
- [12] Y. Han, J. Wang, W. Li, R. Ma, and X. Jin, "Oil film variation and surface damage in the process of reciprocation-oscillation transformation," *Tribology International*, vol. 140, p. 105828, Jun. 2019, doi: [10.1016/j.triboint.2019.06.021](https://doi.org/10.1016/j.triboint.2019.06.021).
- [13] G. I. Kelbaliyev and S. R. Rasulov, *Hydrodynamics and Mass Transfer in Dispersed Media*. Moscow: Khimizdat, 2019.
- [14] A. A. Burkov and S. A. Pyachin, "Formation of WC-Co coating by a novel technique of electrospark granules deposition," *Materials & Design (1980-2015)*, vol. 80, pp. 109–115, May 2015, doi: [10.1016/j.matdes.2015.05.008](https://doi.org/10.1016/j.matdes.2015.05.008).
- [15] Y. Yao and Y. Zhou, "Effects of deep cryogenic treatment on wear resistance and structure of GB 35CRMOV steel," *Metals*, vol. 8, no. 7, p. 502, Jun. 2018, doi: [10.3390/met8070502](https://doi.org/10.3390/met8070502).